

Metallic nature of metal-molecule interface formed by Au-Se bonds

Kazumichi Yokota,¹ Masateru Taniguchi,^{1,2,*} Hiroyuki Tanaka,¹ and Tomoji Kawai¹

¹*Nanoscience and Nanotechnology Center, The Institute of Scientific and Industrial Research, Osaka University, Osaka 567-0047, Japan*

²*PRESTO, Japan Science and Technology Agency (JST), Honcho, Kawaguchi, Saitama 332-0012, Japan*

(Received 27 February 2008; published 15 April 2008)

Scanning tunneling microscopy (STM) images revealed that the adsorbate structure of a monolayer film of benzeneselenolate molecules on gold is represented by the Au(111) $2\sqrt{7} \times \sqrt{3}$ herringbone structure. The adsorbate structure that is obtained by STM measurements matches the optimized structure that is obtained by first-principles calculations. First-principles calculations of the gold-benzeneselenolate interface revealed that electronic states near the Fermi level were formed from the highest occupied molecular orbital of the isolated benzeneselenolate molecules and suggested that electron transfer and electron transport easily occur across the metal-molecule interface that is formed by Au-Se bonds. We propose that this metal-molecule interface is useful for fabricating molecular devices.

DOI: [10.1103/PhysRevB.77.165416](https://doi.org/10.1103/PhysRevB.77.165416)

PACS number(s): 68.43.Hn, 68.37.Ef, 73.20.At

I. INTRODUCTION

The functions of molecule-based devices that have a metal-molecule interface, such as organic electroluminescence devices (ELs),^{1,2} organic field-effect transistors (OFETs),^{1,3} and nanoscale molecular devices,⁴ depend not only on the electronic structures of individual organic molecules, their crystals, and their thin films but also on the electronic structure of the metal-molecule interface. In the case of an EL and an OFET, the charge injection energy barrier from the metal to the molecule is affected by the alignment of the highest occupied molecular orbital (HOMO) or the lowest unoccupied molecular orbital (LUMO) level of the molecules with respect to the metal Fermi level. The charge injection energy barrier is an important parameter that controls the luminescence efficiency in an EL and the field-effect mobility in the OFET. We note that the charge injection energy barrier is not the only parameter that controls the luminescence efficiency, as it is also dependent on the interfacial electronic coupling strength.^{1,2} On the other hand, the field-effect mobility also depends on the chemical interaction between the metal and molecules and the interface state.^{1,3}

Furthermore, when the device size is reduced to a single molecular level, the metal-molecule interface has the greatest influence on the device performance.^{4,5} The charge injection energy barrier depends on the energy difference between the Fermi level and the HOMO (or LUMO) level, such that a low charge injection energy barrier yields a high conductance at low bias. However, the charge injection energy barrier also depends on the strength of the electrode-molecule coupling, and an appropriate electrode-molecule coupling results in a high electric conductance, which contributes to the low power consumption of nanoscale molecular devices.⁵ Thus, the device functions are sensitive not only to the alignment of the molecular orbitals with respect to the metal's Fermi energy but also to the electronic structure of the metal-molecule interface. As a result, understanding the electronic structure of the metal-molecule interface is extremely important to control the properties of molecule-based devices.

Since the discovery of self-assembled films, Au-S bonds have been widely used for metal-molecule bonding.⁶ However, it is difficult to identify the structure of self-assembled films that are formed by Au-S bonds, and the electrode-

molecule interface that are formed by Au-S bonds is not ideal for molecular devices because the barrier against charge injection from the electrode to the molecule is high.⁷ Recently, we used C₆H₅SH (benzenethiol), C₆H₅SeH (benzeneselenol), and (C₆H₅Te)₂ (diphenylditelluride) to fabricate monolayer molecular films on Au(111) and evaluated the bonding states and interface electronic states of the Au-S, Au-Se, and Au-Te bonds by using photoelectron spectroscopy.⁸ Although the C₆H₅Te-Au interface could not be evaluated because C₆H₅Te is oxidized during the measurement, the densities of states at the C₆H₅S-Au interface and the C₆H₅Se-Au interface increase to -1.2 and -0.9 eV, respectively, from the Fermi level, which indicates that the electronic states of the metal-molecule interface are able to be controlled by simply changing one of the connecting atoms.

In the present work, we performed scanning tunneling microscopy (STM) on a monolayer film of benzeneselenolate molecules on Au(111) to determine the morphology and electronic structure of the metal-molecule interface that is formed by Au-Se bonds. The images revealed a highly ordered monolayer molecular film of benzeneselenolate on Au(111). The adsorbate structure that is obtained by first-principles calculations matched the structure that is observed in the STM images, and the electronic structure calculations suggest that the density of states that originates from the adsorbate molecules lies at the Fermi level. We propose that the metal-molecule interface that is created by the Au-Se bonds is suitable for molecular devices.

II. EXPERIMENTAL DETAILS

Experiments and calculations were conducted as follows: We obtained a clean Au(111) surface after repeated sputtering and annealing cycles in ultrahigh vacuum (UHV) ($<10^{-7}$ Pa) in the preparation chamber. A monolayer film of benzeneselenolate molecules was deposited on a Au(111) substrate by exposing a single crystal Au(111) substrate to benzeneselenol vaporized under 1.3×10^{-5} Pa for 10 min with a separation of 6 cm between the source of the vapor molecules and the substrate. During fabrication of the monolayer molecular film, the adsorbate molecules were moni-

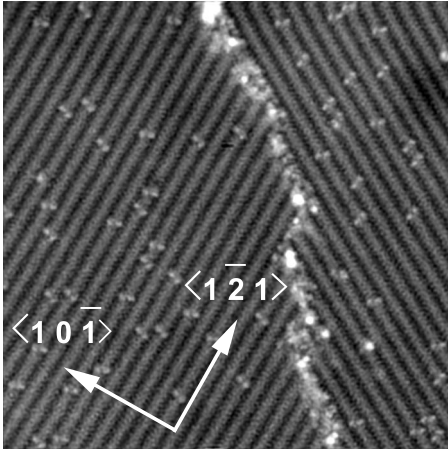


FIG. 1. STM images ($V_s=1.5$ V, $I_t=2$ pA, $x=y=40$ nm, and $z=0.1$ nm) of a monolayer of benzeneselenolate molecules on Au(111).

tored by a mass spectrometer that was positioned near the Au substrate, with peaks observed at molecular masses of 158 ($C_6H_5^{80}SeH$), 156 ($C_6H_5^{78}SeH$), and 154 ($C_6H_5^{76}SeH$). The substrate was then placed in a UHV-STM ($<10^{-7}$ Pa) chamber and observed by STM at a low temperature of 80 K. A tungsten tip was used as an STM probe, and the tunneling current used was 2.0 pA.

A structural optimization of the adsorbate structure of benzeneselenolate on Au(111) was performed by using the density functional theory (DFT) method that was based on the obtained STM images. The system that was used in the calculations was a monolayer of benzeneselenolate molecules on four atomic layers of Au(111), in which the adsorbate structure was modeled as a slab structure measuring 30 Å perpendicular to the Au(111) surface. The coordinates of the Au atoms in the lower two layers were fixed in the bulk positions in the structural optimization calculation. The electronic structure calculations were performed by the DFT method by using Perdew–Burke–Ernzerhof exchange–correlation functionals that were obtained by the generalized gradient approximation.^{9,10} The double-numeric quality basis set with polarization functions was used for the valence electrons, and the effective potentials incorporating relativistic effects were used for the inner shells of the heavy species.^{9,10} Previous studies have reported that the optimized structure of molecules adsorbed on heavy metals is independent of the exchange–correlation functionals and that calculations by using effective potentials incorporating relativistic effects for the inner shells of the heavy species are essential to obtain a structure that is consistent with the experimental observation.¹¹ All calculations were performed by using the DMOL3 program.

III. RESULTS AND DISCUSSION

The STM images show a highly ordered two-dimensional periodic structure of benzeneselenolate (Fig. 1). Because of the similar reaction characteristics of thiol and selenol^{12,13} and from spectroscopic measurements,⁸ benzeneselenolate (C_6H_5Se) adsorbs on Au(111) by forming Au–Se bonds. The

structure originating from the Au(111) surface reconstruction^{14–16} that was often observed in metal–molecule interfaces formed by Au–S bonds is not visible, and the benzeneselenolate has formed a regular array along the $\langle \bar{1}21 \rangle$ direction of the Au(111). The adsorbate structure that is visible in the regions on the left and right of Fig. 1 are mirror images of each other and are equivalent adsorbate structures. Because different regions show identical adsorbate structures, the structure formation is not unique to a particular region. This structure is considered to be the most stable morphology of the adsorbate structure of benzeneselenolate on Au(111) under the experimental conditions that are used in this research. Furthermore, the STM images show spots that are brighter than the regular matrix of benzeneselenolate, with several of these bright spots appearing at the boundaries in the left and right regions. Since the STM images show that bright spots have a higher apparent height than the homogeneous layers, the spots could not be due to the effect of vacancies. Although the origin of the spots has been an open question, the argument on the structure and electronic structure of the homogeneous layers is not hindered by the spots because the homogeneous structure occupied the great portion of the structure on a Au(111) surface.

Figure 2(a) shows an STM image of the left region of the image that is shown in Fig. 1. The lattice shown in the diagram is the unit cell of the adsorbate lattice, as determined from the reciprocal lattice of Fig. 2(a). Figure 2(a) shows that a highly oriented periodic structure is formed by the adsorbate molecules. The unit cell of this periodic structure has lattice constants of $a=1.52$ nm, $b=0.48$ nm, and $\gamma=70.2^\circ$. This structure is an extremely close match to the Au(111) $2\sqrt{7} \times \sqrt{3}$ supercell ($a=1.52$ nm, $b=0.50$ nm, and $\gamma=70.9^\circ$). The formation of this kind of adsorbate structure indicates that the surface stabilization energy after adsorption is even larger than the stabilization energy of the Au(111) surface reconstruction,^{14–16} and this is considered to be due to the strong Au–Se bond. The STM image [Fig. 2(b)] shows that the rows of benzeneselenolate molecules that are observed along the $\langle \bar{1}21 \rangle$ direction form a herringbone structure. Figure 2(d) is the cross section along the line segment AB, as indicated in Fig. 2(b), which shows pairs of benzeneselenolate molecules that are separated by a distance of 0.59 nm repeated at an interval of 1.52 nm. The line segment AB is along the direction of the a axis of the unit cell, and the intermolecular separation of the two benzeneselenolate molecules that are contained in the unit cell is 0.59 nm. High-bias [$V_s=1.5$ V, Fig. 2(c)] and low-bias [$V_s=0.25$ and 0.05, Figs. 2(a) and 2(b)] measurements showed no bias voltage dependence in the STM images. When dI/dV measurements were performed over the molecular layer, the dI/dV spectrum showed no energy gap around the Fermi level, which confirms the metallic character of the molecular layer.

Modeling of the benzeneselenolate adsorbate structure was performed based on the results that were obtained by STM to investigate the adsorbate structure of benzeneselenolate on Au(111) and the electronic structure at the Au–benzeneselenolate interface. From the STM images, the Au(111) $2\sqrt{7} \times \sqrt{3}$ structure was chosen as the unit cell, and two benzeneselenolate molecules with different adsorption

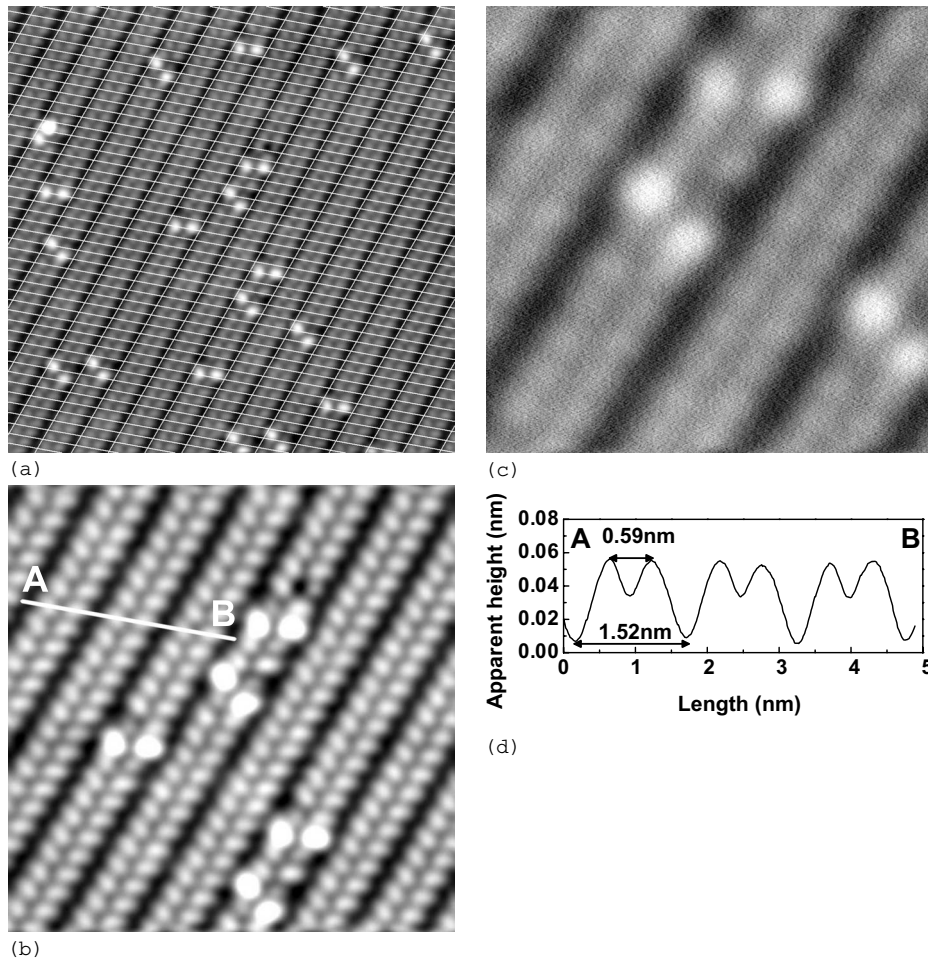


FIG. 2. Structure of a benzeneselenolate monolayer molecular film on Au(111). (a) An expanded image ($V_s=0.25$ V, $I_t=2$ pA, $x=y=20$ nm, and $z=0.1$ nm) of the left side of Fig. 1. The lattice shows the unit cell ($a=1.52$ nm, $b=0.48$ nm, and $\gamma=70.2^\circ$) of the adsorbate structure that is obtained from the reciprocal lattice diagram. (b) STM image ($V_s=0.05$ V, $I_t=2$ pA, $x=y=10$ nm, and $z=0.06$ nm) and (c) one ($V_s=1.5$ V, $I_t=2$ pA, $x=y=5$ nm, and $z=0.09$ nm) of benzeneselenolate monolayer molecular film. (d) Cross section across AB that is indicated in Fig. 2(b).

states were placed within the cell. Furthermore, by considering the intermolecular spacing of 0.59 nm that was obtained from the STM images and the configuration of the molecules within the unit cell, the adsorption sites of the two benzeneselenolate molecules that were contained in the unit cell were deduced as the face-centered-cubic (fcc) and the hexagonal-close-packed (hcp) centroid sites of the unit cell, wherein the spacing between these two centroid sites is 0.60 nm. The adsorbate structure of benzeneselenolate was therefore thought to be the fcc-hcp model wherein each of the two benzeneselenolate molecules I and II within the unit cell adhered to the fcc site and hcp site, respectively, or the hcp-fcc model wherein they adhered to the hcp site and fcc site, respectively. The Au(111) $2\sqrt{7} \times \sqrt{3}$ structure includes ten fcc sites and ten hcp sites, and we obtained optimized structures that were inconsistent with the STM images when a combination of fcc and hcp sites that differed from ours was chosen as the initial model structure.

The results of the structural optimization calculations are shown in Fig. 3 and Table I. The spacing between the Se and Au atoms was 2.67–2.70 Å for Se-Au1 and Se-Au2, 3.08 and 3.05 Å for Se-Au3 on the hcp site, and 3.14 and 3.20 Å for Se-Au3 on the fcc site. In both models, the interatomic spacing of Se-Au3 was longer than that of Se-Au1 and Se-Au2 by approximately 14% for the hcp site and approximately 18% for the fcc site, such that the Se adsorption site formed a bridge site offset from the centroids of the fcc site

and the hcp site. Furthermore, the angle between the Se-C bond and the Au(111) surface was approximately 45° in the fcc-hcp model and 44.5° and 50.5° in the hcp-fcc model. The benzene rings form a structure that overlays the $\langle 1\bar{2}1 \rangle$ direction of the herringbone structure, and the top view of the optimized structure that is shown in Fig. 3 matches the STM images that are shown in Figs. 1 and 2. The total energy difference between the fcc-hcp model and the hcp-fcc model is 49 meV, with no major differences visible between the electronic states and band structures of the two models.

Figure 4(a) shows the band structure and the partial density of states of the adsorbate molecules ($2C_6H_5Se$) and metal substrate (Au) near the Fermi level in the optimized structure. Figure 4(b) shows the frontier molecular orbitals at

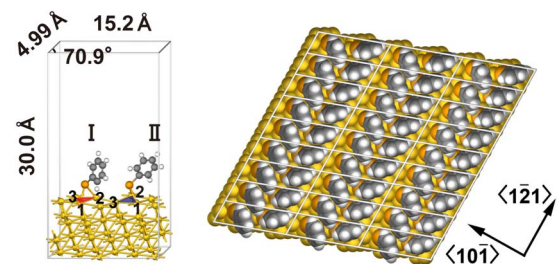


FIG. 3. (Color online) The optimal structure obtained by first-principles calculations and the top view of that structure. 1, 2, and 3 atoms show the gold ones.

TABLE I. Spacings between the Se and Au atoms and angles between the Se-C bond in the optimized structure. In the fcc-hcp model, each of the two benzeneselenolate molecules I and II within the unit cell adhere to the fcc site and hcp site, respectively, while in the hcp-fcc model, they adhere to the hcp site and fcc site, respectively. bf and bh denote that the Se adsorption site forms a bridge site offset from the centroids of the fcc site and the hcp site, respectively.

| Site | fcc-hcp model | | hcp-fcc model | |
|--------------------|---------------|--------|---------------|--------|
| | I(bf) | II(bh) | I(bh) | II(bf) |
| Se-Au1 (Å) | 2.69 | 2.68 | 2.68 | 2.70 |
| Se-Au2 (Å) | 2.67 | 2.67 | 2.67 | 2.70 |
| Se-Au3 (Å) | 3.14 | 3.08 | 3.05 | 3.20 |
| C-Se-Au(111) (deg) | 45.6 | 45.4 | 44.5 | 50.5 |

the Γ point. In Fig. 4(a), band A is the band that originates from the LUMO at the Γ point, and the electron density of this band is localized within the Au, Se, and C-C σ bonds. Band B is the band that originates from the HOMO at the Γ point, and because the electron density of this band is localized in the Au substrate, band B has a wide band dispersion of 1.4 eV that crosses the Fermi level, with the metallic Au substrate properties strongly reflected in band B. Bands C and D are bands that originate from HOMO-1 and HOMO-2 at the Γ point, and these orbitals are delocalized over the entire Au substrate and benzeneselenolate molecules. The molecule side of both of these orbitals has the properties of the HOMO of isolated benzeneselenolate molecules. Bands C and D, which originate from the HOMO of benzeneselenolate, are not mutually intersecting but have a bandwidth of approximately 1.5 eV that crosses the Fermi level. When identical electronic structure calculations were performed on a structure that consists only of benzeneselenolate by remov-

ing the metal atoms from the structure in Fig. 3, the energy dispersion of the benzeneselenolate HOMO was found to be 0.05 eV. In other words, the wide bandwidth of bands C and D does not arise from interactions among benzeneselenolate molecules but arises due to interorbital interactions between the HOMO of benzeneselenolate and Au orbitals near the Fermi level via the Au-Se bond. The result of the interactions between these orbitals, as can be seen in the partial density of states ρ of the adsorbate molecules ($2C_6H_5Se$) in Fig. 4(a), is that the density of states that originates from the p orbitals, which forms the nonlocalized molecular orbitals of the molecule, occurs near the Fermi level.

Bands C and D, which originate from the HOMO of benzeneselenolate, have a wide bandwidth and exhibit the characteristic of crossing the Fermi level, facilitating electron transfer and electron transport from the metal to the molecules. This is thought to be the cause of the absence of bias voltage dependency in the STM images, with both the observed periodic structure and electronic states of the experimental results from STM matching the calculation results from first-principles calculations. In other words, metal-molecule interfaces that are formed by Au-Se bonds are metallic one.

IV. SUMMARY

STM images of a monolayer of benzeneselenolate molecules on Au(111) showed that the benzeneselenolate formed an adsorbate structure with the Au(111) $2\sqrt{7} \times \sqrt{3}$ structure, and this adsorbate structure matched the adsorbate structure that was obtained by first-principles calculations. Electronic structure calculations of the interface revealed that the electronic states near the Fermi level of the metal-molecule interface that was formed by Au-Se bonds was formed from molecular orbitals that originates from the HOMO of the

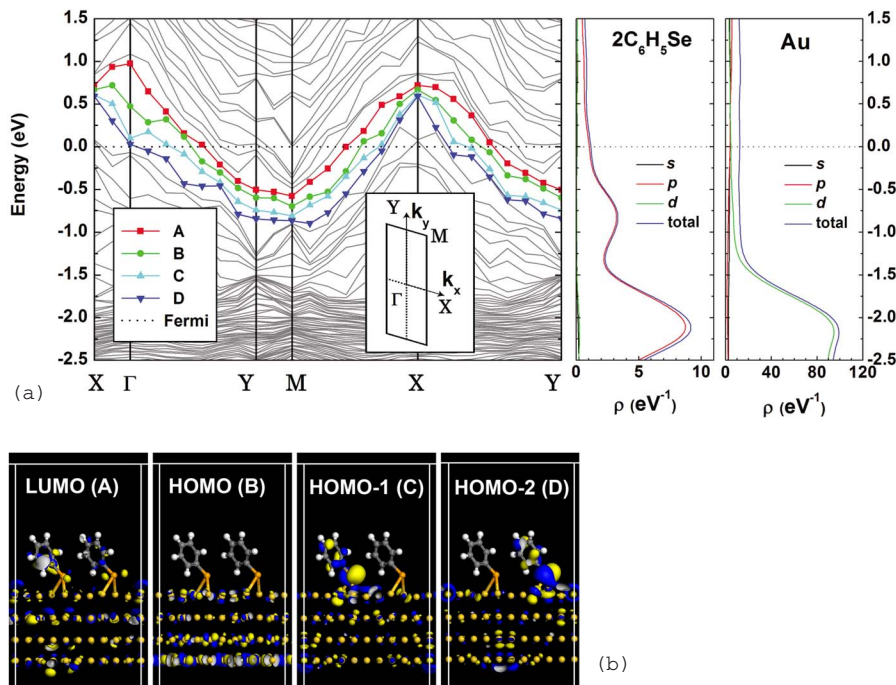


FIG. 4. (Color online) Electronic structure of benzeneselenolate on Au(111). (a) Band structure and partial density of states of adsorbate molecules ($2C_6H_5Se$) and gold (Au) in the optimized structure of benzeneselenolate on Au(111). $E=0$ eV represents the Fermi level. (b) Frontier molecular orbitals at the Γ point. Blue and yellow within the diagram show the ± 0.025 isosurfaces of the molecular orbitals.

adsorbate molecules. The metal-molecule interface that is formed by Au-Se bonds is a metallic one and is predicted to be able to reduce the device operating voltages. The Au-Se bond is therefore thought to be an effective metal-molecule interface for controlling the device characteristics of molecular devices.

ACKNOWLEDGMENTS

Financial support for the present work has been provided in part by a Grant-in-Aid for Scientific Research on Priority Areas "Electron transport through a linked molecule in nanoscale" from the Ministry of Education, Culture, Sports, Science and Technology of Japan.

*Author to whom correspondence should be addressed. FAX: +81-6-6875-2440. taniguti@sanken.osaka-u.ac.jp

¹X.-Y. Zhu, *Surf. Sci. Rep.* **56**, 1 (2004).

²W. R. Salaneck, S. Stafström, and J. L. Brédas, *Conjugated Polymer Surfaces and Interfaces: Electronic and Chemical Structure of Interfaces for Polymer Light Emitting Devices* (Cambridge University Press, New York, 1996).

³H. Siringhaus, *Adv. Mater. (Weinheim, Ger.)* **17**, 2411 (2005).

⁴R. L. McCreery, *Chem. Mater.* **16**, 4477 (2004).

⁵S. Datta, *Electronic Transport in Mesoscopic Systems* (Cambridge University Press, Cambridge, 1995).

⁶A. Ulman, *Chem. Rev. (Washington, D.C.)* **96**, 1533 (1996).

⁷M. DiVentra and N. D. Lang, *Phys. Rev. B* **65**, 045402 (2001).

⁸K. Yokota, M. Taniguchi, and T. Kawai, *J. Am. Chem. Soc.* **129**, 5818 (2007).

⁹M. Dolg, U. Wedig, H. Stoll, and H. Preuss, *J. Chem. Phys.* **86**, 866 (1987).

¹⁰A. Bergner, M. Dolg, W. Kuechle, H. Stoll, and H. Preuss, *Mol. Phys.* **80**, 1431 (1993).

¹¹H. Orita, N. Itoh, and Y. Inada, *Chem. Phys. Lett.* **384**, 271 (2004).

¹²K. T. Camon and L. G. Hurley, *J. Phys. Chem.* **95**, 9979 (1991).

¹³C. A. Szafranski, W. Tanner, P. E. Laibinis, and R. L. Garrell, *Langmuir* **14**, 3570 (1998).

¹⁴L. Strong and G. M. Whitesides, *Langmuir* **4**, 546 (1988).

¹⁵Y.-T. Kim, R. L. McCarley, and A. J. Bard, *J. Phys. Chem.* **96**, 7416 (1992).

¹⁶A.-A. Dhirani, R. W. Zehner, R. P. Hsung, P. Guyot-Sionnest, and L. R. Sita, *J. Am. Chem. Soc.* **118**, 3319 (1996).